Polymer Journal, Vol. 37, No. 9, pp. 686–693 (2005)

Synthesis and Characterization of UV-Induced Interpenetrating Polymer Network (IPN) Structure of Poly(urethane acrylate) (UA Polymer)/Silica Hybrids

Tomoki OGOSHI,[1] Yoshiki CHUJO,[1,†] and Akira ESAKI[2]

[1]*Department of Polymer Chemistry, Graduate School of Engineering, Kyoto University,*
Katsura, Nishikyo-ku, Kyoto 615-8510, Japan
[2]*Mitsubishi Chemical Group Science and Technology Research Center, INC.,*
1000, Kamoshida-cho, Aoba-ku, Yokohama 222-8502, Japan

(Received February 16, 2005; Accepted June 13, 2005; Published September 15, 2005)

ABSTRACT: High transparent and homogeneous poly(urethane acrylate) (UA Polymer)/silica hybrids were obtained by using strong ionic interaction between carboxylic acid groups of the UA Polymer and amino moieties of silica resulting from 3-aminopropyltriethoxysilane (APTEOS). The ionic interaction was directly confirmed by FT-IR measurement. The homogeneity of the obtained UA Polymer/silica hybrids was examined by SEM, TM-AFM and nitrogen adsorption porosimetry studies. Thermal property of the polymer hybrids was also checked by TGA study. Furthermore, the *semi*-interpenetrating polymer network (*semi*-IPN) structured UA Polymer/silica hybrids, where UA Polymer was dispersed in silica gel matrix, were changed to the IPN structured polymer hybrids by photo-induced cross-linking between UA Polymers. The change of the surface hardness, solvent-resistant property, and surface roughness on nanometer scale depending on the formation of IPN structure was investigated. [DOI 10.1295/polymj.37.686]

KEY WORDS Organic-Inorganic Polymer Hybrids / Sol–Gel Reaction / Poly(urethane acrylate) / IPN Structure / Solvent-Resistant Property / Silica Gel /

Organic-inorganic polymer hybrids based on the ambient sol–gel technology have attracted tremendous attentions and been expanding in various fields because of their interesting new properties.[1–27] The elaborated organic-inorganic polymer hybrids exhibited both organic and inorganic features. Furthermore, the novel properties such as superior transparency,[28] excellent solvent-resistance,[13,15,17,18] flame-retardancy, high gas-barrier property[19] and surface-hardness[14] are added due to the nanometer scale miscibility between organic polymer and inorganic materials.

To prepare transparent polymer hybrids based on the sol–gel approach,[29] the affinity between organic polymer and inorganic oxide is necessary. The poor compatibility between organic polymer and inorganic silica gel results in the formation of the micro-scale composite. The introduction of the covalent bond[24–27] and physical interactions into the interface between organic polymer and inorganic silica gel is valuable and useful methodology. Our group has prepared organic-inorganic polymer hybrids utilizing physical interactions such as hydrogen bond,[22,23] aromatic[20] and ionic[21] interactions between organic polymer and silica gel. The structure of the constructed polymer hybrids is *semi*-interpenetrating polymer network (*semi*-IPN), in which organic polymer chains are embedded in silica gel matrix at nanometer level. Furthermore, the *semi*-IPN structure was stepwise changed to IPN structure by cross-linking between organic polymer chains in silica gel matrix.[15,18] The solvent-resistant property of polymer hybrids is dramatically improved by the formation of IPN structure due to the strong interpenetration between organic polymer gel and silica gel. The stepwise IPN formation is useful methodology in order to change the properties of the polymer hybrids. In addition, we recently reported the simultaneous IPN formation: Organic polymer gel was prepared *in-situ* during the formation of silica gel matrix from sol–gel process.[13,17] The *in-situ* IPN formation gave the transparent polymer hybrids by controlling the gelation rate between organic polymer gel and silica gel even in the poor compatibility between organic polymer and silica gel.

Here in this article describes the stepwise UV-induced IPN formation of poly(urethane acrylate) (UA Polymer)/silica hybrids. UA Polymer consists of urethane backbone, carboxylic acid groups at side chain and radically reactive acrylate moieties at both end-sides. Therefore, UA Polymer forms three dimensional network by UV-inducing cross-linking reaction of acrylate moieties. UA polymer was soft segments and widely applied for various industrial fields such as coatings, adhesives and fibers. In the present research, we hybridize “soft” UA Polymer with “hard” silica gel at a nanometer level due to the reinforcement of UA Polymer. For the preparation of transparent

---

[†] To whom correspondence should be addressed (E-mail: chujo@chujo.synchem.kyoto-u.ac.jp).

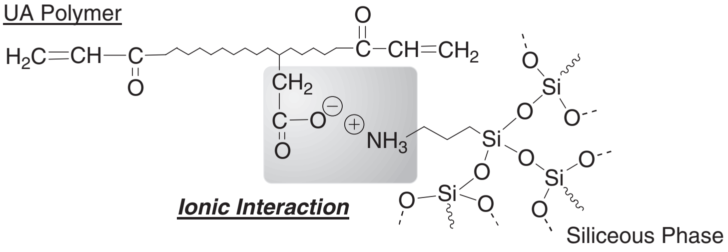

Scheme 1.

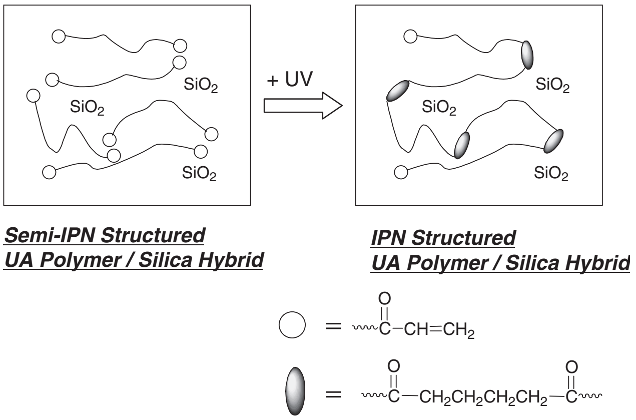

Scheme 2.

polymer hybrids, the strong ionic interaction between acrylic acid groups of the UA Polymer and amino moieties from 3-aminopropyltriethoxysilane (APTEOS) was employed as a physical interaction (Scheme 1). The transparency of the obtained polymer hybrids was gradually improved according to the increase of APTEOS used. The structure of the obtained polymer hybrids was changed from *semi*-IPN to IPN structure with the UV light irradiation (Scheme 2). Changes of surface-hardness, topography of the surface at the nanometer level, thermal and solvent-resistant properties depending on the formation of IPN structure were revealed in details. Preparation of UV-setting urethane resin/silica hybrids utilizing ionic interaction is first example and they will be promisingly applied for the resist materials because their parts within UV irradiation formed IPN structure, which showed strong thermal and solvent resistant properties.

EXPERIMENTAL

Materials

Poly(urethane acrylate) (UA Polymer) ($M_w = 3000$) was obtained from Mitsubishi Chemical Corporation. UA Polymer consists of urethane main-chain, carboxylic acid groups at side chain and acrylate moieties at both end-sides. Tetramethoxysilane (TMOS) was distilled and stored under nitrogen atmosphere. The other solvents and reagents were used as supplied.

Measurements

Thermogravimetric analysis (TGA) was performed using a TG/DTA6200, SEIKO Instruments, Inc., with heating rate of 10 °C min^{-1} in air. Scanning electron microscopy (SEM) measurements were conducted using a JEOL JNM-5310/LV system. The surface images were measured using a tapping mode atomic force microscopy (TM-AFM) (SPA 400, SEIKO Instruments) operating at room temperature. Height and phase images were recorded simultaneously. Nanoprobe cantilevers (SI-DF20, SEIKO Instruments) were utilized. The FT-IR spectra were obtained using a Perkin Elmer 1600 infrared spectrometer. Nitrogen adsorption porosimetry was conducted with a BEL Japan Inc.

Synthesis of UA Polymer/Silica Hybrids

Typical preparation procedure of polymer hybrids with UA Polymer is as follows. UA Polymer was dissolved in DMF. To the mixture, prescribed amount of tetramethoxysilane (TMOS), APTEOS and 0.1 M aqueous hydrochloric acid were added. Then, the resulting solution was stirred for 2 h at room temperature in a sealed bottle to proceed sol–gel reaction. Then, the photo-radical initiator of 1-hydroxycyclohexyl phenyl ketone (5 wt % to UA Polymer) was dissolved in the solution under a dark condition. The mixture was placed in a polypropylene container covered with an aluminum foil having a few pinholes and left in an oven at 60 °C. After the complete removal of the solvent, the glassy polymer hybrids were obtained.

UV-Induced Interpenetrating Polymer Network (IPN) Formation

Formation of IPN structured polymer hybrids was induced by the irradiation of UV light from 175W Xe lamp filtered with a Toshiba UV-D33S glass filter. The reaction was performed at room temperature.

Solvent-Resistant Property of UA Polymer/Silica Hybrids

The powdered hybrids were extracted with solvents (methanol and tetrahydrofuran (THF)) using Soxhlet apparatus for 3 d. After the solvent-extraction, the

Table I. Synthesis of UA Polymer/Silica Hybrids

run	UA Polymer (mg)	TMOS (mg)	APTEOS (μL)	Solvent (mL)	0.1 M $HCl_{aq.}$ (mL)	appearance
1[a]	500	2500	—	acetone 5	1.2	phase separated
2[a]	500	2500	—	MeOH 5	1.2	phase separated
3[b]	500	1000	—	DMF 5	0.2	phase separated
4[b]	500	—	1000	DMF 5	0.2	transparent
5[b]	500	1000	1000	DMF 5	0.2	transparent
6[b]	500	100	500	DMF 5	0.2	transparent
7[b]	500	—	500	DMF 5	0.2	transparent
8[b]	500	—	300	DMF 5	0.2	transparent
9[b]	500	—	100	DMF 5	0.2	transparent
10[a]	500	—	1000	MeOH 5	0.2	translucent

[a] Stirring time was 2 h and the mixture was left at room temperature in air. [b] Stirring time was 2 h and the mixture was heated at 60 °C in air.

Table II. Synthesis of UA Polymer/Silica Hybrids[a]

run	UA Polymer (mg)	TMOS (mg)	APTEOS (μL)	DMF (mL)	appearance	ceramic yield (wt %) calcd.	ceramic yield (wt %) obsd.[b]
11	500	1000	—	5	phase separated	—	—
12	500	1000	6.3	5	phase separated	—	—
13	500	1000	12.5	5	translucent	—	—
14	500	1000	25	5	transparent	44.8	32.4
15	500	1000	50	5	transparent	45.2	47.0
16	500	1000	100	5	transparent	46.0	45.7
17	500	1000	150	5	transparent	46.7	44.6

[a] 0.2 mL of 0.1 M HCl aq. was used as a catalyst. Stirring time was 2 h and the mixture was heated at 60 °C in air. [b] Measured by TGA.

samples were dried in a vacuum oven at 100 °C. The amount of remained organic component in the hybrids was estimated by TGA measurement in air.

Nitrogen Adsorption Porosimetry

The powder of polymer hybrids was heated at 600 °C in an ambient atmosphere for 24 h to remove organic components. After the calcination, the sample was dried in a vacuum oven at 100 °C. The sample was dried at 150 °C for 2 h at reduced pressure before porosimetry measurements. The surface area was calculated with the Brunauer–Emmet–Teller (BET) equation[30] in the range of 0.05 to 0.30 (p/p_0) and the pore size distribution was estimated by the Barrett–Joyner–Halenda (BJH) method.[31]

RESULTS AND DISCUSSION

Synthesis of UA Polymer/Silica Hybrids Using Ionic Interaction

Polymer hybrids with UA Polymer were prepared using TMOS and APTEOS as a silica gel source. The results are shown in Table I. The samples using TMOS brought about phase separation (run 1–3). On the other hand, the transparent polymer hybrids were obtained by employing APTEOS (run 4–9), indicating that APTEOS was necessary for the preparation of transparent polymer hybrids. The effect of APTEOS contents on the homogeneity of polymer hybrids with UA Polymer was then examined (Table II). As shown in Table II, the sample without APTEOS, the obtained composite was vivid phase separated (run 11, the photograph of the sample is shown in Figure 1a). The

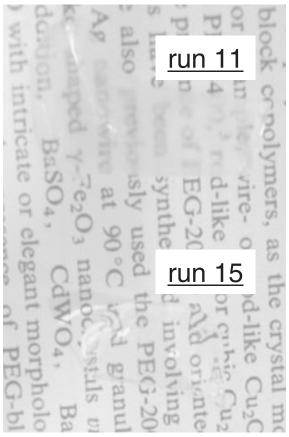

Figure 1. Photographs of (a) the sample without APTEOS (run 11) and (b) the polymer hybrid with APTEOS (run 15).

transparency of the obtained polymer hybrids was gradually increased according to the increase of the amount of APTEOS used (run 12, 13). With further addition of APTEOS, the obtained polymer hybrids were completely transparent (run 14–17, photograph; Figure 1b), indicating that the UA Polymer was mixed in siliceous network in the order of nanometers. From these observations, the strong ionic interaction between carboxylate anion moieties of UA polymer and ammonium cation groups of siliceous phase enables the preparation of transparent UA Polymer/silica hybrids. The formation of silica gel was checked by TGA measurement. The ceramic yields observed by TGA were almost equal to that calculated, therefore the quantitative formation of silica gel matrix was confirmed.

The miscibility between UA Polymer and silica gel was examined by SEM and TM-AFM measurements. In the sample without APTEOS, large aggregations were clearly observed (run 11, Figure 2a). The white parts indicate silica domain. In case of the obtained composite with small amount of APTEOS (12.5 μL, run 13), the miscibility between UA Polymer and silica was improved compared with the sample without APTEOS (run 11). Nevertheless, the heterogeneous aggregations of silica phase were observed at 7000 magnifications (Figure 2b). The high roughness was also found in the height image of TM-AFM (Figure 3a). In contrast, the polymer hybrid with large amounts of APTEOS (50 μL, run 15) exhibited no images at 15000 magnifications (Figure 2c) and the surface was smooth (Figure 3b), strongly indicating the nanometer-scale miscibility between UA Polymer and siliceous phase.

(a) run 11 (without APTEOS)

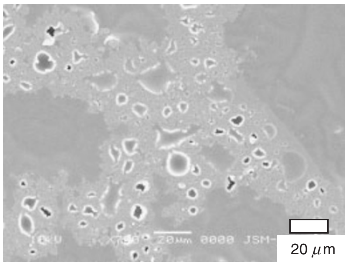

(b) run 13

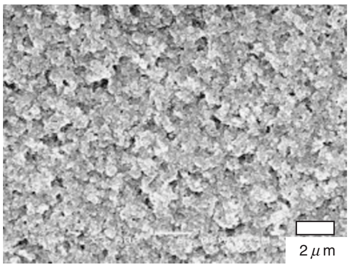

(c) run 15

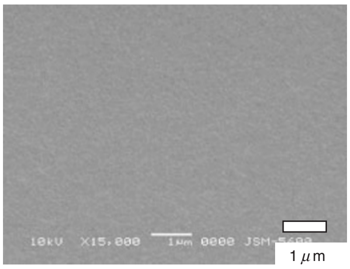

Figure 2. Scanning electron microscope images of (a) the composite without APTEOS (run 11, the scale bar: 20 μm), (b) the sample with 12.5 μL of APTEOS (run 13, the scale bar: 2 μm) and (c) the polymer hybrid with 50 μL of APTEOS (run 15, the scale bar: 1 μm).

Evidence of Formation of Ionic Interaction between UA Polymer and Siliceous Phase

The ionic interaction between carboxylate anion moieties of the UA Polymer and ammonium cation moieties of silica was revealed by FT-IR measurement. As shown in Figure 4a, the peak of C=O stretching vibration was observed at 1712 cm^{-1} in UA Polymer. The peak was identified as the carboxylic acid group of UA Polymer. On the other hand, the UA Polymer/silica hybrid (run 4) exhibited new peak at 1561 cm^{-1}, resulting from carboxylate anion groups of UA Polymer (Figure 4b). These results

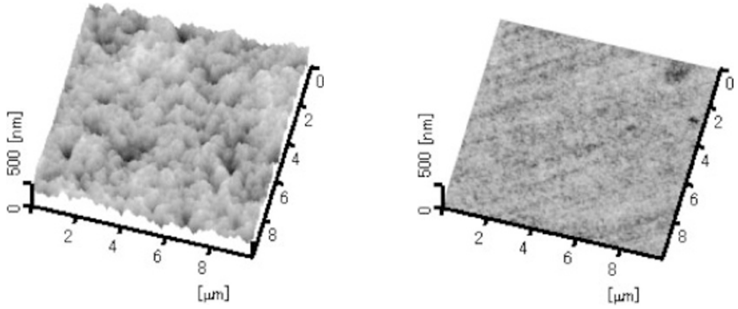
(a) run 13

(b) run 15

Figure 3. Tapping mode atomic force microscope (TM-AFM) images of (a) the sample with 12.5 μL of APTEOS (run 13) and (b) the polymer hybrid with 50 μL of APTEOS (run 15).

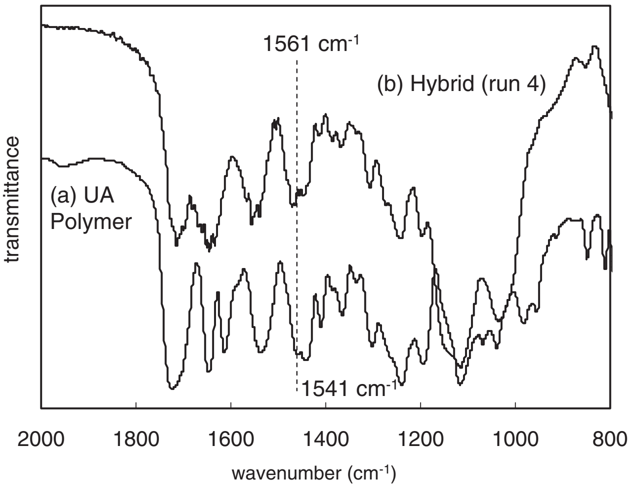

Figure 4. FT-IR spectra of (a) the original UA Polymer and (b) the polymer hybrid (run 4).

clearly confirm the proton transfer from the carboxylic acid groups of UA Polymer to amino groups of silica gel and the formation of the ionic bonds.

Nitrogen Adsorption Porosimetry Study

The miscibility of UA Polymer/silica hybrids was quantitatively estimated by nitrogen adsorption porosimetry study. As shown in Scheme 3, the porous silica was obtained by burning out organic component at 600 °C from polymer hybrids without any shrinking of silica gel matrix. The silica gel matrix is so rigid and hard that the size of the obtained pore silica should reflect the domain of organic polymer, as justified this methodology in previous papers.[12,16,17,21,23] Adsorption isotherm curve of the porous silica obtained by calcination of the UA Polymer/silica hybrid (run 14) is shown in Figure 5. The curve showed high adsorption of nitrogen gas in low pressure and the large histolysis around $p/p^0 = 0.75$, which was classified type IV curve and indicated the presence of the nano-pores. The obtained porous silica had large pore volume (124.1 mL/g) and surface area (540 m^2/g) calculated from BET. Pore size distribution of the porous silica was estimated by BJH method (Figure 6). The pore was observed below 5 nm (the peak top of the pore size was 4.1 nm), which strongly indicates the nanometer scale dispersion of the UA Polymer in silica gel matrix.

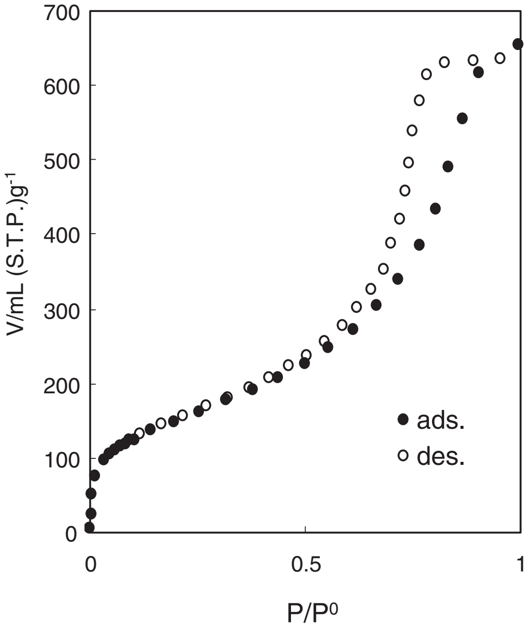

Figure 5. Adsorption isotherm curve of the porous silica obtained by calcination of the UA Polymer/silica hybrid (run 14).

Thermal Study of UA Polymer/Silica Hybrids

Thermal property of the UA Polymer/silica hybrids was checked by TGA measurement (Figure 7). The curve of weight loss of the UA Polymer/silica hybrid (run 15) was shifted to high temperature compared to the pristine UA Polymer. Ten weight percentage loss temperature (T_{10}) of the UA Polymer/silica hybrid and UA polymer was 264.1 and 159.6 °C, respectively, suggesting that the thermal stability of UA Polymer was extremely improved by hybridization with silica gel at the nanometer level.

Solvent-Resistance of UA Polymer/Silica Hybrids Depending on the Extraction Solvents and the Ionic Bond Points

The effect of the points of the ionic bond and the kinds of the extraction solvents on the solvent-resistant property of the UA Polymer/silica hybrids was

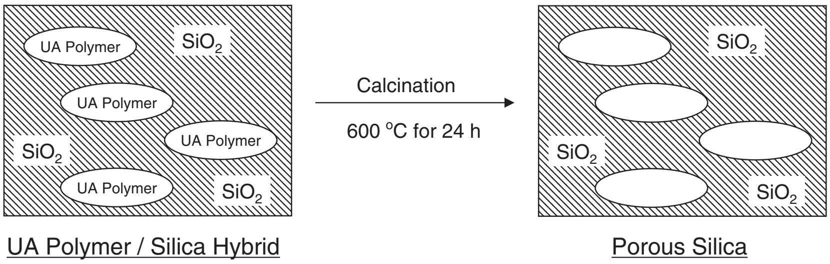

Scheme 3.

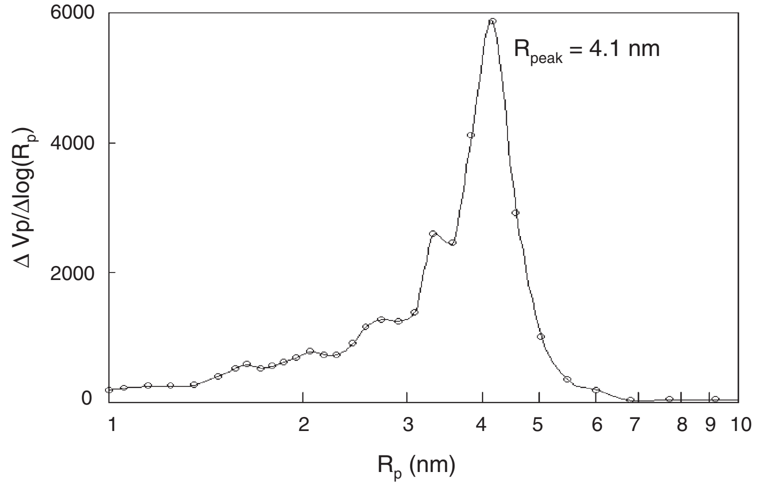

Figure 6. Pore size distribution plot of the porous silica obtained by calcination of the polymer hybrid (run 14).

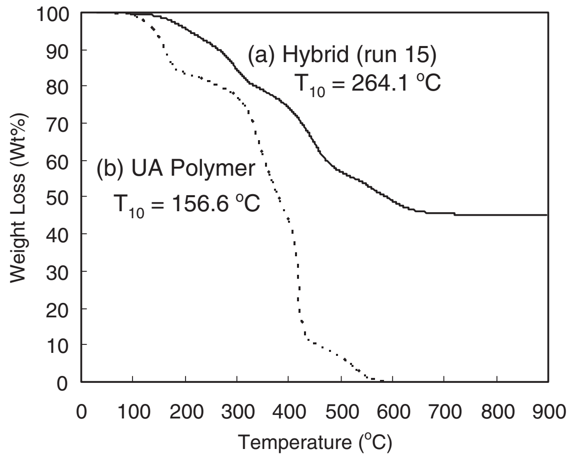

Figure 7. TGA study of (a) the polymer hybrid (run 15) and (b) the UA Polymer.

Table III. Solvent Extraction Efficiency of UA Polymer/Silica Hybrids

run	UA Polymer (mg)	TMOS (mg)	APTEOS (μL)	extraction efficiency (%)[a]	
				MeOH	THF
15	500	1000	50	67.2	52.3
16	500	1000	100	60.8	30.2
17	500	1000	150	50.9	8.5

[a] The polymer content of the polymer hybrids before (p_b) and after (p_a) the extraction was calculated from TGA in air, and the solvent extraction efficiency (E) was calculated according to the equation: $E = 100(p_b - p_a)/p_b(100 - p_a)$.

investigated. The trends were clearly found as shown in Table III. The UA Polymer/silica hybrids exhibited the high solvent-resistance for THF compared with that for methanol. In the polar solvent (methanol), the ionic bond between carboxylic acid of the UA Polymer and amino groups of silica gel was easily weakened and the large amounts of the UA Polymer were extracted from the polymer hybrids. In contrast, the ionic bond was extremely strong in the non-polar solvents (THF). Regarding the effect of the numbers of the ionic bond points in the polymer hybrids, the solvent-extraction efficiency was gradually decreasing according to the increasing of the ionic bond points. The multipoint ionic bonds between UA Polymer and silica gel prevented the extraction of the UA Polymer from the polymer hybrids. Especially, the solvent-resistance for THF was remarkably improved compared with that for methanol by increasing the ionic bond points. These observations resulted from the low ability of cleavage of the ionic bond by THF extraction compared with that by methanol extraction.

Formation of IPN Structured UA Polymer/Silica Hybrids Induced by UV Light Irradiation

IPN structured UA Polymer/silica hybrids were synthesized by UV-induced cross-linking reaction between UA Polymer chains in silica gel matrix. The photo-radical initiator of 1-hydroxycyclohexyl phenyl ketone was added during the preparation of UA Polymer/silica hybrids for the proceeding of radical cross-linking reaction between UA Polymers. All the obtained polymer hybrids were transparent and homogeneous even if the photo-radical initiator was contained in the polymer hybrids (Table IV). Next, IPN structured UA Polymer/silica hybrids were induced by UV light irradiation. The transparency of UA Polymer/silica hybrids was not changed after UV irradiation. Surface roughness depending on UV irradiation on the nano meter scale was measured by TM-AFM (Figure 8). Before UV irradiation, the polymer hybrid was extremely smooth (Figure 8a). But, the small particles at the nanometer scale clearly appeared on the smooth surface after UV irradiation (Figure 8b). The observation of the nanoparticles resulted from the

Table IV. Synthesis of IPN Structured UA Polymer/Silica Hybrids by UV Light Irradiation[a]

run	UA Polymer (g)	APTEPOS (μL)	TMOS (g)	appearance	surface hardness before UV	surface hardness after UV
4	40	80	—	transparent	3B	1H
6	50	50	10	transparent	1H	3H
UA Polymer		—	—	transparent	—	3B

[a] 10 wt % of photo-initiator, 1-hydroxycyclohexyl phenyl ketone was used.

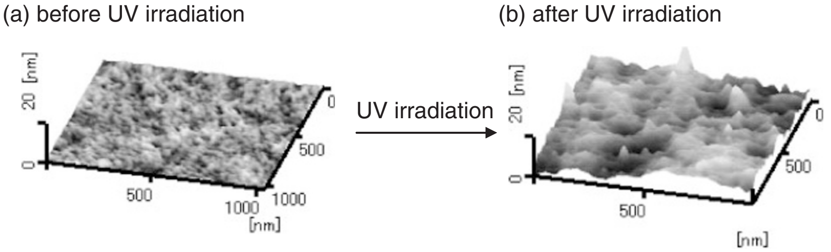
(a) before UV irradiation

(b) after UV irradiation

Figure 8. Tapping mode atomic force microscope (TM-AFM) images of the UA Polymer/silica hybrid (a) before UV irradiation and (b) after UV irradiation.

shrinking of UA Polymer segment by cross-linking. Regarding the surface hardness of polymer hybrids depending on UV light irradiation, the results are summarized in Table IV. In run 4 (before UV irradiation), the surface hardness measured by pencil was 3B. The polymer hybrid using TMOS and APTEOS (run 6) showed high surface hardness (1H) compared with run 4, indicating that the surface hardness was improved by containing high siliceous segment. The surface hardness was extremely changed by UV light irradiation. The surface hardness of run 4 and run 6 was changed to 1H and 3H, respectively. From these observations, the proceeding of the cross-linking between UA Polymer chains by UV irradiation was strongly suggested.

For the further elucidation of the IPN structured polymer hybrids by UV irradiation, the solvent extraction experiment was carried out. If the photo-induced cross-linking reaction of UA Polymer chain took place in silica gel matrix, the solvent extraction of UA Polymer from silica gel matrix would be strongly inhibited due to the three dimensional interpenetration between UA Polymer network and silica gel. The crushed polymer hybrids were extracted with methanol for 3 d. The solvent extraction efficiency of the UA Polymer in polymer hybrids was calculated by TGA measurement (Figure 9). In the UV-untreated polymer hybrid (run 15, Figure 9a), the ceramic yield at 900 °C increased compared with the ceramic yield before the solvent extraction, indicating that large amounts of UA Polymer were extracted from the polymer hybrid. The solvent extraction efficiency was 79.1%. On the other hand, little increasing of ceramic yield was found (Figure 9b) in the UV-irradiated polymer hybrid (The extraction efficiency was 9.0%). The strong interpenetration between three dimensional UA Polymer network induced by UV irradiation and silica gel efficiently prevented the

(a) UV-Untreated UA Polymer / Silica Hybrid (run 14)

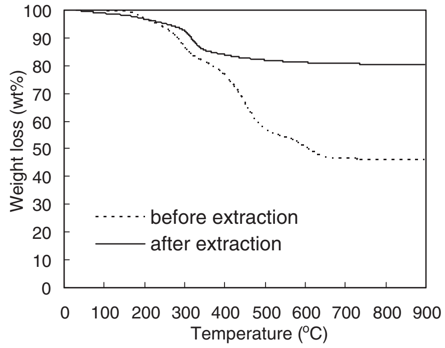

(b) UV-irradiated UA Polymer / Silica Hybrid (run 14)

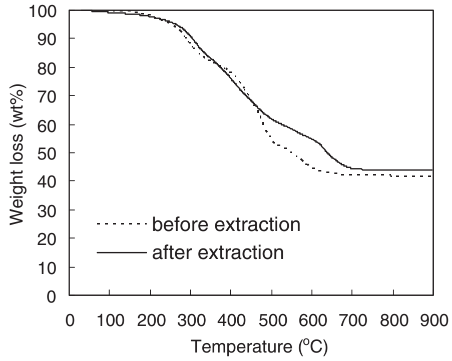

Figure 9. TGA traces of (a) the UV-untreated UA Polymer/silica hybrid (run 14) and (b) the UV-irradiated UA Polymer/silica hybrid.

solvent extraction of the UA Polymer from the polymer hybrid.

CONCLUSIONS

UA Polymer/silica hybrids were prepared *via* the formation of strong ionic bond between carboxylic acid groups of UA Polymer and amine moieties from APTEOS. The nanometer scale homogeneity of the obtained UA Polymer/silica hybrids was revealed by SEM, TM-AFM and nitrogen adsorption porosimetry studies. The thermal stability of UA Polymer was dramatically improved by nanometer scale reinforcement with silica gel. Furthermore, the IPN formation between three dimensional UA Polymer network and silica gel induced upon UV light irradiation gave excellent solvent-resistance and surface hardness compared with the *semi*-IPN structure.

REFERENCES

1. J. Wen and G. L. Wilkes, *Chem. Mater.*, **8**, 1667 (1996).
2. D. A. Loym and K. J. Shea, *Chem. Rev.*, **95**, 1431 (1995).
3. B. M. Novak, *Adv. Mater.*, **5**, 422 (1993).
4. E. P. Giannelis, *Adv. Mater.*, **8**, 29 (1996).
5. Y. Chujo and R. Tamaki, *MRS Bull.*, **26**, 389 (2001).
6. I. Ichinose and T. Kunitake, *Chem. Rec.*, **2**, 339 (2002).
7. C. Sanchez, F. Ribot, and B. Lebeau, *J. Mater. Chem.*, **9**, 35 (1999).
8. J. J. E. Moreau and M. W. C. Man, *Coord. Chem. Rev.*, **178**, 1073 (1998).
9. B. J. Lebeau and C. Sanchez, *Curr. Opin. Solid State Mater. Sci.*, **4**, 1 (1999).
10. a) Special issues for nanocomposites materials., *Chem. Mater.*, **8**(8) (1996).
    b) Special issues for nanocomposites materials., *Chem. Mater.*, **9**(11) (1997).
    c) Special issues for nanocomposites materials., *Chem. Mater.*, **13**(10) (2001).
    d) Special issues for nanocomposites materials., *MRS Bull.*, **26**(5) (2001).
11. T. Ogoshi and Y. Chujo, *Macromolecules*, **37**, 5916 (2004).
12. T. Ogoshi and Y. Chujo, *Macromolecules*, **36**, 654 (2003).
13. T. Ogoshi, H. Itoh, K. M. Kim, and Y. Chujo, *Macromolecules*, **35**, 334 (2002).
14. T. Ogoshi, T. Fujiwara, M. Bertolucci, G. Galli, E. Chiellini, Y. Chujo, and K. J. Wynne, *J. Am. Chem. Soc.*, **126**, 12284 (2004).
15. Y. Imai, H. Itoh, K. Naka, and Y. Chujo, *Macromolecules*, **33**, 4343 (2000).
16. R. Tamaki and Y. Chujo, *J. Mater. Chem.*, **8**, 1113 (1998).
17. T. Ogoshi, H. Itoh, K. M. Kim, and Y. Chujo, *Polym. J.*, **35**, 178 (2003).
18. Y. Imai, K. Naka, and Y. Chujo, *Polym. J.*, **30**, 990 (1998).
19. R. Tamaki, Y. Chujo, K. Kuraoka, and T. Yazawa, *J. Mater. Chem.*, **8**, 1741 (1999).
20. R. Tamaki, K. Samura, and Y. Chujo, *Chem. Commun.*, 1131 (1998).
21. R. Tamaki and Y. Chujo, *Chem. Mater.*, **5**, 1113 (1998).
22. Y. Chujo, E. Ihara, S. Kure, and T. Saegusa, *Macromolecules*, **26**, 5681 (1993).
23. Y. Chujo, H. Matsuki, S. Kure, T. Saegusa, and T. Yazawa, *J. Chem. Soc., Chem. Commun.*, 635 (1994).
24. Y. Wei, D. Jin, D. J. Brennan, D. N. Rivera, Q. Zhuang, N. J. DiNardo, and K. Qiu, *Chem. Mater.*, **10**, 769 (1998).
25. S. Wang, Z. Ahmad, and J. E. Mark, *Chem. Mater.*, **6**, 943 (1994).
26. Y. Wei, D. C. Yang, and L. G. Tang, *Makromol. Chem., Rapid Commun.*, **14**, 273 (1993).
27. Q. Wang, N. Liu, X. Wang, J. Li, X. Zhao, and F. Wang, *Macromolecules*, **36**, 5760 (2003).
28. C. F. Bohren and D. R. Huffman, "Absorption and Scattering of Light by Small Particles," Wiley, New York, N.Y., 1983, p 3.
29. C. J. Brinker and G. W. Scherer, "Sol–Gel Science, The Physics and Chemistry of Sol–Gel Processing," Academic Press Inc., San Diego, CA, 1990, p 97.
30. S. Brunauer, P. H. Emmett, and E. Teller, *J. Am. Chem. Soc.*, **60**, 309 (1938).
31. E. P. Barrett, L. G. Joyner, and P. P. Halenda, *J. Am. Chem. Soc.*, **73**, 373 (1951).